Environmental Science & Technology Letters

Letter

pubs.acs.org/journal/estlcu

Microbial Rechargeable Battery: Energy Storage and Recovery through Acetate

Sam D. Molenaar,*[,†,‡] Annemerel R. Mol,[‡] Tom H. J. A. Sleutels,[†] Annemiek ter Heijne,[‡] and Cees J. N. Buisman[†,‡]

[†]Wetsus, European Centre of Excellence for Sustainable Water Technology, Oostergoweg 9, 8911 MA Leeuwarden, The Netherlands

[‡]Department of Environmental Technology, Wageningen University, Bornse Weilanden 9, 6708 WG Wageningen, The Netherlands

Supporting Information

ABSTRACT: Bioelectrochemical systems hold potential for both conversion of electricity into chemicals through microbial electrosynthesis (MES) and the provision of electrical power by oxidation of organics using microbial fuel cells (MFCs). This study provides a proof of concept for a microbial rechargeable battery (MRB) allowing storage of electricity by combining MES and a MFC in one system. Hexacyanoferrate(II/III) was used as counter redox couple. Duplicate runs showed stable performance over 15 days, with acetate being the main energy carrier. An energy density of around 0.1 kWh/m^3 (normalized to anode electrolyte volume) was achieved at a full cycle energy efficiency of 30−40%, with a nominal power output during discharge of 190 W/m^3 (normalized to anode volume). With this study, we show a new potential application area for bioelectrochemical systems as a future local energy storage device.

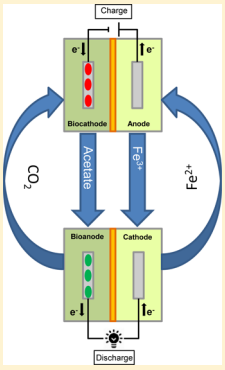

INTRODUCTION

With ever increasing worldwide energy demands and concerns about the environmental impact of burning fossil fuels that have been raised, renewable energy sources are slowly but steadily gaining ground.[1] One of the major challenges for implementing renewable electricity is the variability in the generation of sun and wind energy and matching this with a fluctuating demand. Models predict that, as long as shares of renewables remain below 30% of the total electricity supplied to the grid, through smart grid technologies, dynamics in power grid demand and supply might be balanced without additional energy storage capacities.[2] However, energy storage devices will likely become a necessity with a further increase in renewable electricity shares. Conventional energy storage systems like lithium batteries, compressed air energy storage (CAES), pumped hydro technology, and newer technologies such as sodium ion batteries will likely play their role to this end. Current storage systems often cope with safety issues (CAES) or toxicities (heavy metals), allowing their use only under precisely controlled conditions, require scarce and nonrenewable materials, or can be used only in suitable geographic environments (pumped hydro).[3] Therefore, a safe, renewable, and low-cost system for household-scale energy storage would hold great potential. Bioelectrochemical systems (BESs) could play an important role in future energy storage, as the catalysts in these systems (i.e., microorganisms) (re)generate and use renewable and widely available substrates, namely, water, CO_2, and nutrients.

While both microbial electrosynthesis (MES) and microbial fuel cells (MFCs) have been the subject of intensive study over the past few decades,[4−9] they have, to the best of our knowledge, not yet been integrated into one system, with an objective of storing and recovering electricity. For this new concept, we introduce the name microbial rechargeable battery (MRB). In a MRB, during the MES phase, electrical energy is consumed to form acetate, while during the MFC phase, electrical energy is generated by the consumption of acetate. The proposed system would therefore require stable intermittent operation of a biocathode, a bioanode, and their counter electrodes.

To provide a proof of concept of the MRB, we connected an acetate-producing biocathode (MES) hydraulically to an acetate-oxidizing bioanode (MFC) and operated both in turn with a total charge/discharge cycle period of 24 h (thus matching the day/night rhythm typical for solar energy production). During these cycles, CO_2 was successfully converted into acetate and energy was recovered by subsequent oxidation of the acetate formed (see Figure 1 for a schematic overview). The ferri/ferrocyanide redox couple was used as a reversible reaction at the counter electrodes. We analyze the performance of the MRB in terms of efficiency and stability.

MATERIALS AND METHODS

System Design. Experiments were conducted in duplicate setups, each consisting of two electrochemical cells. One set of

Received: February 12, 2016
Revised: March 8, 2016
Accepted: March 9, 2016

DOI: 10.1021/acs.estlett.6b00051
Environ. Sci. Technol. Lett. XXXX, XXX, XXX−XXX

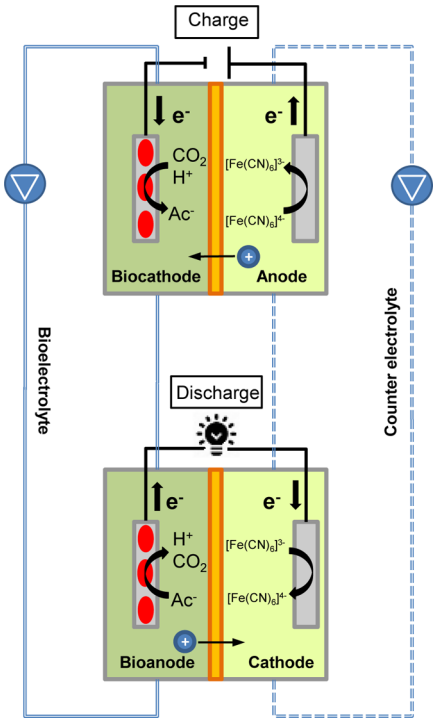

Figure 1. Schematic overview of the microbial rechargeable battery (MRB) consisting of a CO_2-reducing charging cell (MES, top) and an acetate-oxidizing discharging cell (MFC, bottom). Depicted are the (simplified) predominant reactions taking place at the bioanode, biocathode, and their counter electrodes; the flow of electrons (e^-) across the external electrical circuits; and the transfer of cations (+) across the membranes.

cells is further termed a microbial rechargeable battery (MRB). For each MRB, one cell (charging cell) performed MES with an acetate-producing biocathode, while the second (discharging cell) was operated as a microbial fuel cell (MFC) with an acetate-consuming bioanode.

Each cell consisted of two Plexiglas flow compartments (33 cm^3), one flat plate current collector (stainless steel SS316), a flat plate counter current collector (Pt/lrO_2-coated Ti, Magneto special anodes BV, Schiedam, The Netherlands), and two support plates.[10] Electrolytes were separated by a cation exchange membrane (Fumasep FKB-PEEK, Fumatech, projected surface area of 22 cm^2). The bioanode, the biocathode, and their counter electrodes consisted of plain graphite paper and five layers of graphite felt (thickness of 3 mm, FMI Composites Ltd., Galashiels, Scotland) firmly held between the current collector and membrane, completely filling the flow compartments.

Media and Microbial Inoculum. The electrolyte, which was shared by both the bioanode and the biocathode and is further termed the bioelectrolyte, consisted of 0.4 g/L NH_4HCO_3, 0.05 g/L $Ca(OH)_2$, 0.1 g/L $MgSO_4{\cdot}7H_2O$, 9.6 g/L K_2HPO_4, 2.1 g/L Na-2-BES, 4 g/L NaOH, 0.1 mL/L trace metals,[11] and 0.1 mL/L vitamins (DSMZ medium 141). At the start, influent mineral medium was sparged with CO_2 with a resulting initial pH of 6.4. The counter electrolyte was composed of 2.9 g/L $Na_4[Fe(CN)_6]{\cdot}10H_2O$, 21 g/L $K_4[Fe(CN)_6]{\cdot}3H_2O$, 4.0 g/L $K_3[Fe(CN)_6]$, and 1.7 g/L K_2HPO_4 and was kept saturated with CO_2 throughout the experiments. The conductivities of the bioelectrolyte and counter electrolyte were measured at the start to be 1.6 and 2.9 S/m, respectively, thus not limiting current production throughout the experiment.

The bioelectrolyte was inoculated with a combination of (1) effluent from an acetate-producing biocathode (inoculated previously with a mixed culture extracted from an anaerobic digester and cow manure) and (2) effluent from an active MEC running on acetate.

Reactor Start-Up and Operation. Reference electrodes (Ag/AgCl, Prosense, Oosterhout, The Netherlands; +0.203 V vs the standard hydrogen electrode) were connected to the electrolytes. All reported potentials were expressed relative to this reference. Current and power densities are reported to be normalized to bioelectrode volume (33 cm^3) or membrane surface area (22 cm^2). Energy and charge densities are normalized to bioelectrolyte recirculation volume (280 mL). The total counter electrolyte recirculation volume was 2240 mL. All electrolytes were recirculated with a pump speed of 10 mL/min. The bioelectrolyte pH was measured in-line (Endress +Hauser, CP571D-7BV21). The reactor temperature was maintained at 32 ± 1 °C using climate control of the research cabinet. A multichannel potentiostat (N-stat DC, Ivium Technologies, Eindhoven, The Netherlands) was used to perform electrochemical measurements and experiments. Individual cell voltages and membrane potentials were measured using a data logger (RSG40, Endress+Hauser, Reinach, Switzerland) in conjunction with high-impedance potentiometers.

Start-up of the bioanode and biocathode occurred after inoculation and with a continuous supply of medium. Bioanode potentials were controlled at −0.35 V. Biocathodes were current controlled at −750 A/m^3 (−11.3 A/m^2). After stable bioanodic currents were established and maintained for several days (4−6 days), the charge/discharge experiment was started. During the experiment, the two cells of a MRB were switched in turns between open-circuit and controlled current over a total cycle period of 24 h. First, a constant current of −150 A/m^3 (−2.26 A/m^2) was supplied to the biocathode (MES) for 16 h (charging), during which the bioanode (MFC) was placed under open-circuit conditions. The charging period was then followed by discharge for 8 h with the bioanode current controlled at 300 A/m^3 (4.52 A/m^2) and the biocathode placed under open-circuit conditions in turn. During discharge, the bioanode current was maintained until its potential reached −0.35 V, after which the potentiostat was programmed to switch to potential control to maintain this potential. This switch from galvanostatic to potentiostatic operation prevented unintended side reactions from taking place after acetate had been depleted.

Chemical Analysis and Performance Calculations. Liquid samples of bioelectrolytes were taken 15 min prior to the end of each charging and discharging phase. During sampling, sample volumes of 5 mL were replaced by an equal volume of a new CO_2-saturated bioelectrolyte, keeping the total recirculation volume constant. The samples were analyzed for fatty acid content (Dionex UHPLC System). Gas formation was quantified using a gas counter (MGC, Ritter Apparatebau, Bochum, Germany), and the headspace composition was analyzed via gas chromatography (μGC, Varian CP 4900). For a more detailed description of analytical methods, see ref 12.

The overall Coulombic efficiency (overall CE, or CE_{total}) represents the total charge recovered (Q_r) during the

DOI: 10.1021/acs.estlett.6b00051
Environ. Sci. Technol. Lett. XXXX, XXX, XXX−XXX

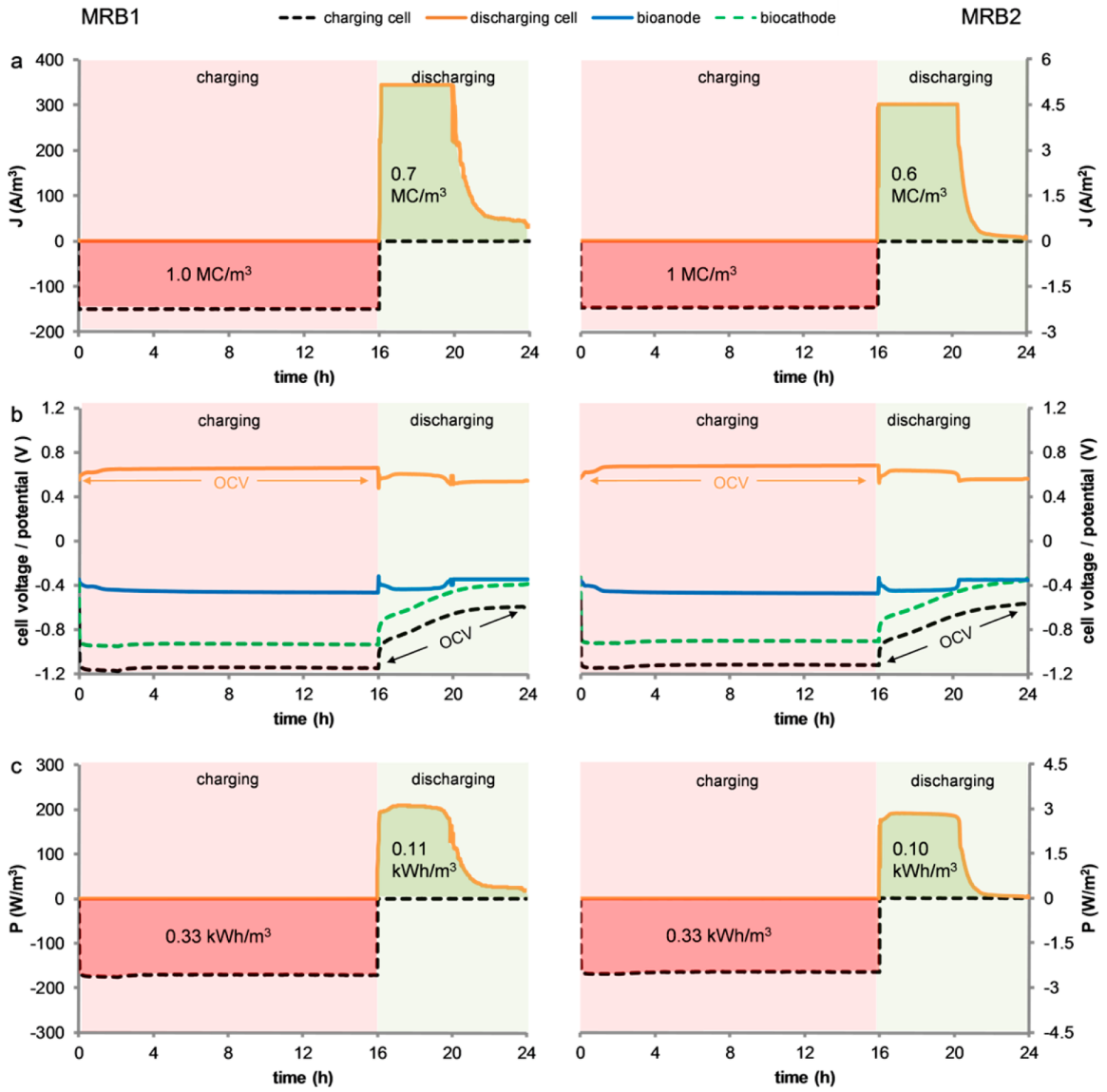

Figure 2. Voltages and potentials (b) and (a) current and (c) power densities as typically observed throughout one cycle for both MRBs. Current and power densities are normalized to both total bioelectrolyte volume (left *y*-axis) and projected (membrane) surface area (right *y*-axis). As patterns throughout cycles showed great similarity, data of the last recorded cycle (no. 15) are depicted. This graph clearly shows the feasibility of a MRB based on acetate/carbonate redox chemistry.

discharging period, compared to the total charge used during the charging period (Q_c):

$$CE_{total} = \frac{Q_r}{Q_c}$$

The maximal fraction of charge recovered through intermediate storage in acetate was then calculated by

$$f_{Q,acetate} = \frac{\Delta c_{acetate} VnF}{Q_r}$$

where $\Delta c_{acetate}$ is the measured concentration difference in acetate between a charged and discharged electrolyte, V the effective electrolyte volume, n the number of electrons involved in acetate oxidation (8), and F the Faraday constant.

The energy efficiency per cycle (EE) was calculated by dividing the integral of power over the discharging period (16–24 h) by the integral of power over the charging period (0–16 h):

$$EE = \frac{\int_{16}^{24} P_{discharge}(t)\,dt}{\int_{0}^{16} P_{charge}(t)\,dt}$$

RESULTS AND DISCUSSION

For each MRB, the charging cell performed MES with an acetate-producing biocathode, while the discharging cell was operated as a MFC with an acetate-oxidizing bioanode. Each cycle started with a charging period of 16 h, during which biocathodes were controlled at −5 mA (2.26 A/m^2). In this period, the potential of both biocathodes was between −0.9 and −1.0 V, a value typical for the formation of hydrogen on graphite.[7] Using ferrocyanide (Fe^{2+}) as an electron donor, this required charging cell voltages of −1.1 to −1.2 V. Data for one

DOI: 10.1021/acs.estlett.6b00051
Environ. Sci. Technol. Lett. XXXX, XXX, XXX−XXX

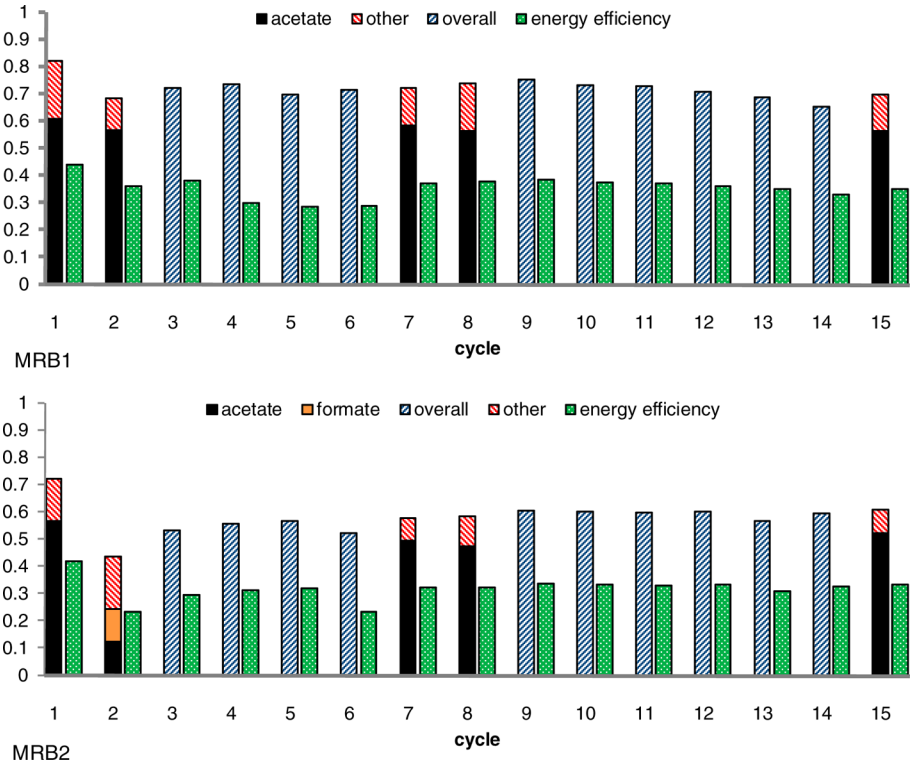

Figure 3. Overall CE (filled bar) throughout charge/discharge cycles for both microbial rechargeable batteries (MRB1 and MRB2). Fractionation between charge recovered through acetate or other (charge carriers) was calculated from measured fluctuations in acetate concentration, assuming a 100% anodic conversion efficiency of acetate to current. For cycles 3−6 and 9−14, no chemical analysis of the electrolytes was performed; thus, for these cycles, the overall CE is displayed without further fractionation.

representative cycle for each MRB are shown in Figure 2, which first shows the applied charging/discharging currents (Figure 2a), followed by the observed cell voltages and electrode potentials (Figure 2b) and resulting power densities (Figure 2c). For a more detailed analysis of all electrode potentials, see Figure S1 of the Supporting Information. During charging, bioanodes were operated under open-circuit conditions, with their open-circuit potential (OCP) decreasing toward −0.5 to −0.55 V. After 16 h, biocathodes were switched to open-circuit and bioanodes were operated as MFC at a constant current of 10 mA (4.52 A/m^2). This resulted in anode potentials of −0.46 to −0.43 V and discharge cell voltages of 0.5−0.6 V, corresponding to a power density of 2.8−3.0 W/m^2 throughout the first few hours of the discharge period. After a few hours, anode potentials showed a marked increase, indicating substrate depletion. When the anode potential increased to values higher than −0.35 V, the potentiostat switched from current control to anode potential control (−0.35 V) and the current decreased rapidly. After the system had been discharged for 8 h, at which point current densities from the bioanodes had dropped to values of <0.5 A/m^2, a new cycle was started. Figure 2 (a and c) also shows the charging capacity (MC/m^3) and energy density (kWh/m^3) during both charge and discharge, represented by the shaded surface areas, from which overall Coulombic efficiency (CE) and energy efficiency were calculated. Cycles were repeated in a stable way for 15 days, illustrating the ability of biocathodes and bioanodes to become active directly after being inactive for 8−16 h (open-circuit) and to be operated intermittently throughout many cycles. No pH adjustments were made throughout the experiments, and only minor pH fluctuations were detected throughout the charge/discharge cycles due to the presence of bicarbonate/carbonic acid and phosphate acting as a buffer. Despite the minor fluctuations in pH, no net gas production was observed during charging or discharging periods in general, indicating inorganic carbon stayed dissolved throughout the experiments. More detailed analysis of pH is provided in the Supporting Information (Figure S2).

Figure 3 shows the charge recovery efficiency for both MRBs, during each cycle of the experiment. Overall CEs, representing the electrons recovered from the bioanode compared to the electrons fed to the biocathode in one cycle, reached 50−80% throughout all cycles except one. Chemical analysis of liquid samples taken at the end of the charging and discharging period showed high selectivity toward acetate as a product of CO_2 reduction, and the contribution of acetate to total stored charge was determined. The level of production of acetate was slightly lower in the first cycles, gradually increasing and then becoming stable in later cycles. Typically, 50−60% of electrons supplied to the biocathode during charging were stored in acetate, corresponding to final acetate concentrations of 0.68 and 0.85 mM.

An exception to the general observations described above was formed by cycle 2 of MRB2, in which the charge recovered in acetate (12%) was lower. Remarkable for this cycle was the production of formate, which in turn accounted for ∼12% of the transferred charge. The produced formate was fully degraded during the subsequent discharge, thus not leading to losses of the overall CE for this cycle. Moreover, during this cycle, measurable amounts of gas were produced, mainly consisting of hydrogen. This way, hydrogen losses accounted for a lower CE during this cycle. Assuming the solution was saturated with hydrogen at the end of this specific cycle (±0.7 mM H_2), dissolved hydrogen could account for a maximum of

DOI: 10.1021/acs.estlett.6b00051
Environ. Sci. Technol. Lett. XXXX, XXX, XXX−XXX

4.5% of charge transfer from the biocathode to the bioanode. In subsequent cycles, these deviations from previous cycles did not reoccur, and mechanisms causing the disturbance in this single cycle were not further investigated.

As the overall charge recovered exceeded the charge stored in acetate in all cycles, the presence of charge carriers other than acetate (as occurring in the bulk electrolyte) was imperative. Headspace hydrogen partial pressures typically reached 3% at full charge, with the remaining part composed of 30% CO_2 and 66% N_2 (no methane detected). No net production of gas was observed during cycles other than those discussed previously, and the low partial pressure of hydrogen and accompanying dissolved hydrogen concentration was not sufficiently high to contribute substantially to the total charge stored. However, it seems plausible that hydrogen was the intermediate in acetate formation, with the biocathode allowing almost full conversion of the produced hydrogen to acetate, in accordance with recent findings.[11] Scanning electron microscopy examination of the electrode material showed only a limited presence of bacteria attached to the biocathodes, while bioanodes possessed well-developed biofilms (Figure S3). Microbial characterization of the obtained biomass was not further pursued at this stage.

An alternative charge carrier, besides H_2 and acetate, could be other organics, or inorganics like sulfate. The role of sulfate was likely limited, as measured sulfate concentrations showed no substantial fluctuations throughout the cycles (data not shown). Alternatively, the unexplained charge recovered could be stored in the anodic biofilm instead of in the bulk electrolyte. Possibly, electrons are transferred to and accumulating in or at the anodic biofilm during the charging phase. The mediator responsible for this electron transfer from the biocathode to the bioanode can be any biologically available redox active compound. The anodic biofilm is presumed to possess a pool of redox mediators in its intercellular environment that, during charging, is gradually reduced while under open-circuit conditions.[13,14] The extent to which this mechanism could play a role was not further investigated and will become less evident when the system is operated at higher energy densities (thus reaching higher acetate concentrations).

In the study presented here, specific energy densities of ~0.1 kWh/m^3 were reached. For the proposed technology to be competitive with conventional batteries, this energy density needs to be increased. A first important factor impacting energy density is the choice of counter electrode. Here, the counter electrode reaction, using hexacyanoferrate, was selected for practical reasons (soluble at neutral pH, reversible reaction, and reasonably high potential). A next step is to find a suitable, reversible, and environmentally attractive counter electrode reaction to further demonstrate the feasibility of the MRB. Finding a better counter electrode reaction has another potential advantage: the overall energy efficiency (n = 30) was on average 33.5% (s = 4.5%). While part of the energy efficiency loss was explained by Coulombic losses (on average 35%; s = 9%; n = 30), the main part was due to voltage losses. These voltage losses are to some extent inevitable as long as hydrogen is required as an intermediate for acetate production, requiring considerable overpotential during charging compared to the obtained anode potential during discharging. Via the selection of a counter redox reaction with a sufficiently high redox potential, the relative difference between the required charging voltage and the obtained discharging voltage may be reduced, positively impacting overall energy efficiency.

Apart from the reaction at the counter electrode, the maximal achievable energy density of the MRB is directly related to the acetate concentration attained during charging as this defines the anodes' charge capacity. Acetate concentrations of 0.75 M reached previously in hydrogenotrophic reactors provide an optimistic perspective[15] regarding further optimization of this parameter.

In conclusion, we have shown here the proof of concept of a microbial rechargeable battery, using a biocathode that produces acetate from electricity and a bioanode converting acetate into electricity. Depending on the acetate concentration that can be achieved, and the counter reaction involved, the MRB could become a suitable, clean, safe, and renewable alternative to existing battery storage systems. As such, the MRB could become an inexpensive local energy storage device in the future.

■ ASSOCIATED CONTENT

Supporting Information

The Supporting Information is available free of charge on the ACS Publications website at DOI: 10.1021/acs.estlett.6b00051.

Figures S1−S3 (PDF)

■ AUTHOR INFORMATION

Corresponding Author

*E-mail: sam.molenaar@wetsus.nl. Telephone: +31 (0)58 284 300.

Notes

The authors declare no competing financial interest.

■ ACKNOWLEDGMENTS

This work was performed in the cooperation framework of Wetsus, European Centre of Excellence for Sustainable Water Technology (www.wetsus.eu). Wetsus is co-funded by the Dutch Ministry of Economic Affairs and Ministry of Infrastructure and Environment, the Province of Fryslân, and the Northern Netherlands Provinces. The authors thank the participants of the Resource Recovery research theme for the fruitful discussions and their financial support.

■ ABBREVIATIONS

MRB, microbial rechargeable battery; BES, bioelectrochemical system; MFC, microbial fuel cell; MES, microbial electrosynthesis cell; Na-2-BES, 2-bromoethanosulfonic acid sodium salt; CE, Coulombic efficiency.

■ REFERENCES

(1) Wüstenhagen, R.; Menichetti, E. Strategic Choices for Renewable Energy Investment: Conceptual Framework and Opportunities for Further Research. *Energy Policy* **2012**, *40* (1), 1−10.

(2) Denholm, P.; Ela, E.; Kirby, B.; Milligan, M. Role of Energy Storage with Renewable Electricity Generation. *Natl. Renew. Energy Lab.* **2010**, 1−61.

(3) Dunn, B.; Kamath, H.; Tarascon, J.-M. Electrical Energy Storage for the Grid: A Battery of Choices. *Science* **2011**, *334* (6058), 928−935.

(4) Sleutels, T. H. J. A.; Ter Heijne, A.; Buisman, C. J. N.; Hamelers, H. V. M Bioelectrochemical Systems: An Outlook for Practical Applications. *ChemSusChem* **2012**, *5* (6), 1012−1019.

(5) Harnisch, F.; Schröder, U. From MFC to MXC: Chemical and Biological Cathodes and Their Potential for Microbial Bioelectrochemical Systems. *Chem. Soc. Rev.* **2010**, *39* (11), 4433−4448.

DOI: 10.1021/acs.estlett.6b00051
Environ. Sci. Technol. Lett. XXXX, XXX, XXX−XXX

(6) Nevin, K. P.; Woodard, T. L.; Franks, A. E.; Summers, Z. M.; Lovley, D. R. Microbial Electrosynthesis: Feeding Microbes Electricity To Convert Carbon Dioxide and Water to Multicarbon Extracellular Organic Compounds. *mBio* **2010**, *1* (2), e00103-10.
(7) Jourdin, L.; Grieger, T.; Monetti, J.; Flexer, V.; Freguia, S.; Lu, Y.; Chen, J.; Romano, M.; Wallace, G. G.; Keller, J. High Acetic Acid Production Rate Obtained by Microbial Electrosynthesis from Carbon Dioxide. *Environ. Sci. Technol.* **2015**, *49* (22), 13566−13574.
(8) Gildemyn, S.; Verbeeck, K.; Slabbinck, R.; Andersen, S. J.; Prévoteau, A.; Rabaey, K. Integrated Production, Extraction, and Concentration of Acetic Acid from CO 2 through Microbial Electrosynthesis. *Environ. Sci. Technol. Lett.* **2015**, *2* (11), 325−328.
(9) LaBelle, E. V.; Marshall, C. W.; Gilbert, J. A.; May, H. D. Influence of Acidic pH on Hydrogen and Acetate Production by an Electrosynthetic Microbiome. *PLoS One* **2014**, *9* (10), e109935.
(10) ter Heijne, A.; Hamelers, H. V. M; Saakes, M.; Buisman, C. J. N. Performance of Non-Porous Graphite and Titanium-Based Anodes in Microbial Fuel Cells. *Electrochim. Acta* **2008**, *53* (18), 5697−5703.
(11) Zehnder, A. J. B.; Huser, B. A.; Brock, T. D.; Wuhrmann, K. Characterization of an Acetate-Decarboxylating, Non-Hydrogen-Oxidizing Methane Bacterium. *Arch. Microbiol.* **1980**, *124* (1), 1−11.
(12) Sousa, J. A. B.; Plugge, C. M.; Stams, A. J. M.; Bijmans, M. F. M. Sulfate Reduction in a Hydrogen Fed Bioreactor Operated at Haloalkaline Conditions. *Water Res.* **2015**, *68*, 67−76.
(13) Uría, N.; Muñoz Berbel, X.; Sánchez, O.; Muñoz, F. X.; Mas, J. Transient Storage of Electrical Charge in Biofilms of Shewanella Oneidensis MR-1 Growing in a Microbial Fuel Cell. *Environ. Sci. Technol.* **2011**, *45* (23), 10250−10256.
(14) Freguia, S.; Rabaey, K.; Yuan, Z.; Keller, J. Electron and Carbon Balances in Microbial Fuel Cells Reveal Temporary Bacterial Storage Behavior during Electricity Generation. *Environ. Sci. Technol.* **2007**, *41* (8), 2915−2921.
(15) Demler, M.; Weuster-Botz, D. Reaction Engineering Analysis of Hydrogenotrophic Production of Acetic Acid by Acetobacterium Woodii. *Biotechnol. Bioeng.* **2011**, *108* (2), 470−474.

DOI: 10.1021/acs.estlett.6b00051
Environ. Sci. Technol. Lett. XXXX, XXX, XXX−XXX